

# Constrained Large Angle Reorientation Manoeuvres of a Space Telescope Using Potential Functions and a Variable Control Gain

Giovanni Mengali <sup>\*</sup> and Alessandro A. Quarta <sup>†</sup>

*University of Pisa, I-56122 Pisa, Italy*

## Abstract

In this paper we study large angle rotational maneuvers of a space telescope with pointing constraints. The spacecraft attitude control design is formulated and solved by means of potential functions, thus simplifying the problem of frequent reorientation maneuvers. A novel approach is proposed, where a time varying control gain is chosen such that its instantaneous value depends both on the spacecraft kinetic energy and on the distance of the spacecraft from the forbidden directions. As a result, the spacecraft is able to reach points in the potential field arbitrarily close to a constraint and to maneuver with autonomous capability of guidance and control. A case study illustrates the effectiveness of the proposed methodology.

## Nomenclature

$\mathbb{E}$	=	quaternions matrix, see Eq. (9)
$k$	=	dimensionless control parameter
$i, j, k$	=	body reference frame unit vectors
$I$	=	principal moment of inertia
$\mathbb{I}$	=	inertia matrix
$M$	=	control torque
$n$	=	unit vector

---

<sup>\*</sup>Associate Professor, Department of Aerospace Engineering, g.mengali@ing.unipi.it. Corresponding author.

<sup>†</sup>Research Assistant, Department of Aerospace Engineering, a.quarta@ing.unipi.it.

$q_i$	=	quaternion (with $i = \{0, 1, 2, 3\}$ )
$O$	=	spacecraft's center-of-mass
$\mathbb{T}$	=	transformation matrix, see Eq. (5)
$\mathcal{T}_B(x, y, z)$	=	body reference frame
$\mathcal{T}_I(X, Y, Z)$	=	inertial reference frame
$t$	=	time
$V$	=	artificial potential
$\delta$	=	slew angle
$\gamma$	=	solar array sun angle, see Eq. (2)
$\eta$	=	dimensionless control parameter
$\boldsymbol{\omega}$	=	spacecraft's angular velocity ( $\omega = \ \boldsymbol{\omega}\ $ )
$\Omega$	=	angular velocity matrix, see Eq. (8)

### *Subscripts*

0	=	initial
$\oplus$	=	Earth
$\delta$	=	depending on attitude
$\omega$	=	depending on angular velocity
$f$	=	final, desired
$\jmath$	=	Jupiter
$\lrcorner$	=	Moon
$P$	=	scientific payload
$\odot$	=	Sun
$SA$	=	solar array
$\star$	=	target
th	=	threshold

### *Superscripts*

$h$	=	high value
$l$	=	low value
$\cdot$	=	time derivative
max	=	maximum
$\wedge$	=	forbidden cone's aperture angle

## Introduction

In some space applications, such as satellite surveillance and communication, a spacecraft must perform accurate pointing and slewing manoeuvres, whereby the spacecraft is rotated along a large angle amplitude trajectory. In many circumstances it is also required that the sensitive payload does not intercept bright objects such as the Sun, Earth and Moon, to avoid possible damage to the optical instruments. The importance of this subject has stimulated an active research, and different approaches have been reported in the literature<sup>(1-5)</sup>.

The ways in which these maneuvers are performed are important and, indeed, a natural choice is to deal with the reorientation problem within a time-optimal framework. In particular, the unconstrained problem has been addressed from different viewpoints<sup>(6,7)</sup>, including the combined case of time and propellant optimization<sup>(8)</sup>. Time-optimal spacecraft slewing maneuvers with path constraints are much more difficult to synthesize. As a matter of fact, inclusion of path constraints requires augmenting the Hamiltonian function with additional terms describing those constraints<sup>(9)</sup>. Even though the resulting problem can, in principle, be tackled using an indirect approach, the path constraints create particularly difficult challenges. For these reasons Melton<sup>(10,11)</sup> has recently proposed resorting to direct methods, which offer the theoretical advantage of easier problem management. However, it is known that an optimal solution of a spacecraft reorientation maneuver, or even a feasible solution, cannot be automatically guaranteed<sup>(10)</sup>. Therefore, often the optimality of a maneuver may be of lesser importance than the capability of actually generating a feasible trajectory using modest computational efforts and simple implementation.

From this viewpoint an interesting option is offered by potential function based methods. These are inspired by robotics control and have been proposed to simplify frequent reorientation maneuvers of spacecraft with autonomous re-targeting capabilities<sup>(12-16)</sup>. An interesting feature of potential function methods is that the control torques are evaluated in closed

form, thus facilitating the on-board implementation with reduced software requirements and clear advantages over other available control systems. However, some limitations have been pointed out that could hinder their practical use. For instance, Ref. [17] emphasized a possible intrinsic disadvantage of potential methods due to the fact that the spacecraft, while avoiding the forbidden directions, moves substantially away from its nominal path. The aim of this paper is to show that the above drawbacks can be circumvented with a suitable choice of both the potential function and the control law. To better explain these points, it is useful to briefly summarize the potential function approach.

Basically, a scalar nonnegative (artificial) potential function is defined so that it has a global minimum at the desired final attitude, and has regions of high potential corresponding to the forbidden directions. The spacecraft controls are then chosen in such a way that the rate of change of the potential is negative. According to the Lyapunov's direct method, this guarantees that the spacecraft dynamics converges towards the desired direction. To simplify the control system design it has been suggested<sup>(12-14)</sup> that the potential gradient be made proportional to the spacecraft kinetic energy through a constant control gain  $k$ . In other terms, the artificial potential function may be formulated by including appropriate terms involving the measured angular velocity components. This is possible because the choice of the artificial potential function is not unique.

Unfortunately, good reorientation capabilities are conflicting with such a simple control law. Indeed, loosely speaking, high values of the control gain correspond to a slow spacecraft movement, whereas small values of  $k$  correspond to rapid reorientation maneuvers. Of course, due to saturation problems, the spacecraft cannot be accelerated up to an arbitrarily high rotational velocity, otherwise the control torques would not be able to slow down the vehicle when it passes near an obstacle or approaches the pointing direction. On the other hand, too high gain values would provide unacceptably long time responses.

The contribution of this paper is to show that a good compromise solution is a time variant control gain whose value depends both on the spacecraft kinetic energy and on the distance from the forbidden directions. The new control law is based on simple physical considerations and permits the spacecraft to reach points in the potential field arbitrarily close to a constraint and to maneuver with autonomous capability of guidance and control.

## Problem Description

Assume that a spacecraft must perform a reorientation maneuver characterized by a payload pointing direction with respect to an inertial reference frame  $\mathcal{T}_I(X, Y, Z)$ . During such a maneuver the spacecraft must avoid different pointing constraints and, at the same time, guarantee a minimum angle between the solar array nominal plane and the Sun-spacecraft direction<sup>(16)</sup>, see Fig. 1.

For mathematical convenience a payload unit vector  $\mathbf{n}_P$  and a solar array unit vector  $\mathbf{n}_{SA}$  are now introduced. Both unit vectors are fixed with respect to the spacecraft's main body. The pointing constraints are specified in terms of  $m \geq 1$  forbidden directions with respect to the inertial frame and serve to avoid that the scientific payload is damaged by bright sky regions, due to the Sun or other celestial bodies, see Fig. 1(a). This is equivalent to guaranteeing that during the whole reorientation maneuver the following constraints are met: 1) the unit vector  $\mathbf{n}_P$  remains outside  $m$  right circular cones generated around the forbidden directions, and 2) the unit vector  $\mathbf{n}_{SA}$  lies inside a suitable right circular cone generated around the Sun-spacecraft direction. For instance, Fig. 1 shows the pointing constraints due to Sun, Earth, Moon and Jupiter. Undesired spacecraft orientations are expressed through mathematical inequalities in the form

$$\delta_i \triangleq \text{Arccos}(\mathbf{n}_P \cdot \mathbf{n}_i) > \hat{\delta}_i \quad \text{for } i = 1, \dots, m \quad (1)$$

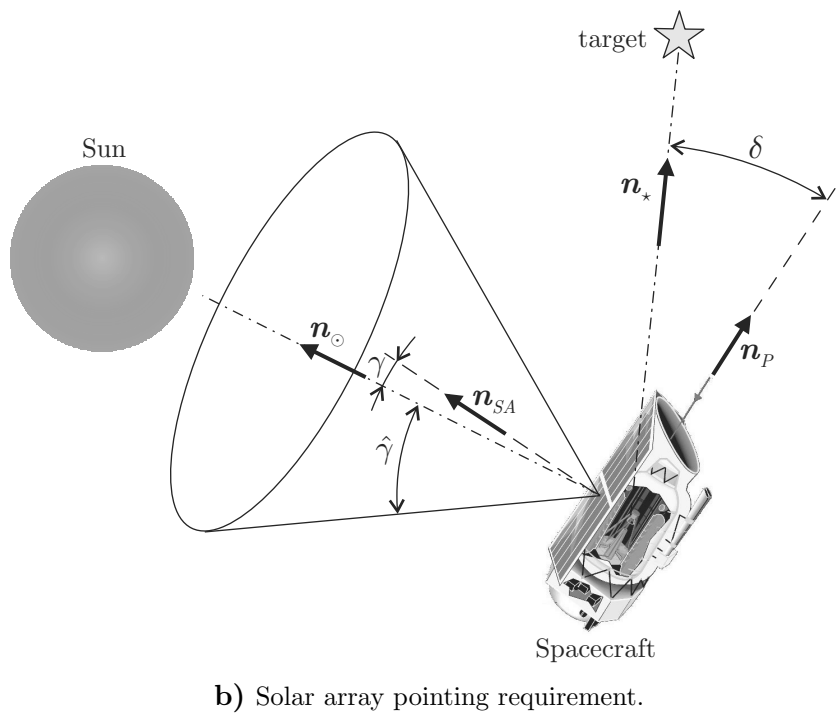
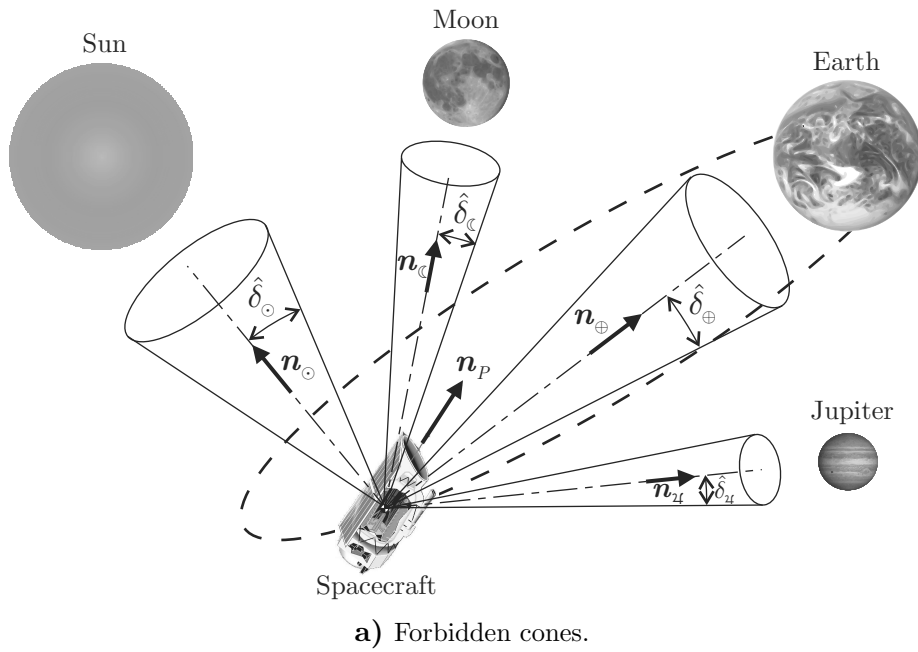


Figure 1: Sketch of the geometric constraints (adapted from Ref. [16]).

whereas the constraint due to the solar array pointing requirement can be written as

$$\gamma \triangleq \text{Arccos}(\mathbf{n}_{SA} \cdot \mathbf{n}_{\odot}) < \hat{\gamma} \quad (2)$$

where  $\hat{\gamma}$  is shown in Fig. 1(b).

Assume that the spacecraft has to align the scientific payload line-of-sight with a target direction (defined through the unit vector  $\mathbf{n}_{\star}$ ) whose components are known in the inertial reference frame  $\mathcal{T}_I$ , see Fig. 1(b). The attitude control law must assure that the target direction is caught and maintained within specified limits. This amounts to stating that, at the end of the reorientation maneuver, both the final angle  $\delta_f$  between the target direction and the scientific payload line-of-sight, and the modulus of the spacecraft's angular velocity  $\|\boldsymbol{\omega}_f\|$  must be sufficiently small, i.e.

$$\delta_f \leq \delta^{\max} \quad \text{and} \quad \|\boldsymbol{\omega}_f\| \leq \omega^{\max} \quad (3)$$

where  $\delta$  is the angle between the directions of  $\mathbf{n}_P$  and  $\mathbf{n}_{\star}$ , viz.

$$\delta \triangleq \text{Arccos}(\mathbf{n}_P \cdot \mathbf{n}_{\star}) \quad (4)$$

In other terms, the problem consists of finding a suitable control law such that the target direction is reached within the prescribed requirements given by Eqs.(3), and the geometric constraints (1)-(2) are met along the whole spacecraft reorientation maneuver.

## Mathematical Model

Consider a body axes reference frame  $\mathcal{T}_B(x, y, z)$  with its origin in the spacecraft's center-of-mass  $O$ , where  $x, y$  and  $z$  are the principal axes of inertia of the spacecraft and let  $\mathbf{i}, \mathbf{j}, \mathbf{k}$

be the corresponding unit vectors. The unit quaternion is chosen to globally represent the spacecraft attitude without singularities<sup>(18)</sup>. Using the Euler's eigenaxis rotation theorem, the angular orientation of  $\mathcal{T}_B$  relative to the inertial frame  $\mathcal{T}_I$  is expressed through the well known transformation matrix  $\mathbb{T}$ :

$$\mathbb{T} = \begin{bmatrix} q_0^2 + q_1^2 - q_2^2 - q_3^2 & 2(q_1 q_2 - q_0 q_3) & 2(q_0 q_2 + q_1 q_3) \\ 2(q_1 q_2 + q_0 q_3) & q_0^2 - q_1^2 + q_2^2 - q_3^2 & 2(q_2 q_3 - q_0 q_1) \\ 2(q_1 q_3 - q_0 q_2) & 2(q_2 q_3 + q_0 q_1) & q_0^2 - q_1^2 - q_2^2 + q_3^2 \end{bmatrix} \quad (5)$$

where  $\mathbf{q} \triangleq [q_0, q_1, q_2, q_3]^T$  is the quaternion unit vector<sup>(6)</sup> associated with  $\mathbb{T}$ . In other terms, if  $\mathbf{w}$  is an arbitrary vector, its components  $[\mathbf{w}]_{\mathcal{T}_B}$  expressed in the body axes reference frame are transformed from  $\mathcal{T}_B$  to  $\mathcal{T}_I$  through the equation:

$$[\mathbf{w}]_{\mathcal{T}_I} = \mathbb{T} [\mathbf{w}]_{\mathcal{T}_B} \quad (6)$$

For the sake of simplicity, in the following the notation  $[\mathbf{w}] \equiv [\mathbf{w}]_{\mathcal{T}_B}$  will be adopted. The Euler's rotational equations of motion for the (rigid) spacecraft, about its center-of-mass  $O$ , are:

$$[\mathbf{M}] = \mathbb{I} [\dot{\boldsymbol{\omega}}] + \boldsymbol{\Omega} \mathbb{I} [\boldsymbol{\omega}] \quad (7)$$

with

$$\mathbb{I} \triangleq \begin{bmatrix} I_x & 0 & 0 \\ 0 & I_y & 0 \\ 0 & 0 & I_z \end{bmatrix} ; \quad \boldsymbol{\Omega} \triangleq \begin{bmatrix} 0 & -\omega_z & \omega_y \\ \omega_z & 0 & -\omega_x \\ -\omega_y & \omega_x & 0 \end{bmatrix} \quad (8)$$



whereas the kinematic equations of angular motion are:

$$[\dot{\mathbf{q}}] = \mathbb{E} [\boldsymbol{\omega}] \quad \text{with} \quad \mathbb{E} \triangleq \frac{1}{2} \begin{bmatrix} -q_1 & -q_2 & -q_3 \\ q_0 & -q_3 & q_2 \\ q_3 & q_0 & -q_1 \\ -q_2 & q_1 & q_0 \end{bmatrix} \quad (9)$$

In Eq. (7), vector  $[\mathbf{M}] \triangleq [M_x, M_y, M_z]^T$  is the total external moment about  $O$ ,  $[\boldsymbol{\omega}] \triangleq [\omega_x, \omega_y, \omega_z]^T$  is the angular velocity of the spacecraft relative to  $\mathcal{T}_I$ , whereas  $I_x$ ,  $I_y$ , and  $I_z$  are the vehicle's principal moments of inertia. In this paper the only external moments are given by the control system, the disturbance torques being negligible.

## Lyapunov-Based Controller

In the following we assume ideal thrusters, capable of generating independent continuous torques along the three principal axes in the range  $[-M_i^{\max}, M_i^{\max}]$ . According to McInnes [13], a continuous control torque can be generated using pulse-width, pulse-frequency modulation of cold gas thrusters. As an alternative, the necessary continuous control torque can also be obtained with electric thrusters. However, in the latter case, a bank of thrusters is probably necessary. In fact, the maximum thrust of a single electric thruster suitable for attitude control usually does not exceed a few hundred millinewtons.

To introduce the control law, consider the state vector  $\mathbf{x} \triangleq [\mathbf{q}^T, \boldsymbol{\omega}^T]^T$  and an artificial potential function, defined as:

$$V(\mathbf{x}) \triangleq V_\delta + V_\omega \quad (10)$$

where

$$V_\delta \triangleq \lambda_1 \frac{\delta^2}{2} \left( f_\gamma + \sum_{i=1}^m f_i \right) \quad (11)$$

$$V_\omega \triangleq \frac{1}{2\eta M^{\max}} [\boldsymbol{\omega}]^T \mathbb{I} [\boldsymbol{\omega}] \quad (12)$$

and

$$f_\gamma = \begin{cases} \frac{1}{\lambda_2 + (\hat{\gamma} - \gamma)^2} & \text{if } \gamma \leq \hat{\gamma} \\ \gamma^2 / (\lambda_2 \hat{\gamma}^2) & \text{if } \gamma > \hat{\gamma} \end{cases} \quad ; \quad f_i = \begin{cases} \frac{1}{\lambda_2 + (\delta_i - \hat{\delta}_i)^2} & \text{if } \delta_i \geq \hat{\delta}_i \\ 2\hat{\delta}_i^2 / [\lambda_2 (\hat{\delta}_i^2 + \delta_i^2)] & \text{if } \delta_i < \hat{\delta}_i \end{cases} \quad (13)$$

In Eqs. (11)–(12)  $\lambda_1$ ,  $\lambda_2$ , and  $\eta$  are dimensionless positive design parameters, and  $M^{\max}$  (which is used to make  $V_\omega$  dimensionless) is the maximum value of the control torques modulus, that is

$$M^{\max} \triangleq \max \{ |M_x^{\max}|, |M_y^{\max}|, |M_z^{\max}| \} \quad (14)$$

Note that both  $V_\delta$  and  $V_\omega$  are functions of the state vector  $\mathbf{x}$ , because  $\delta = \delta(\mathbf{q})$  via Eqs. (4), (5) and (6). Also,  $V(\mathbf{x}) > 0 \forall \mathbf{x} \neq \mathbf{x}_f$  ( $\mathbf{x}_f$  is the target state) and  $V(\mathbf{x}) \rightarrow \infty$  as  $\|\mathbf{x}\| \rightarrow \infty$ .

The artificial potential function (10) is the sum of two terms: the first one ( $V_\delta$ ) depending on the spacecraft attitude [see Eq. (11)] and, in particular, on the position of the scientific payload line-of-sight ( $\delta$ ) or the solar arrays ( $\gamma$ ) with respect to the direction of the pointing constraints and of the target. The second ( $V_\omega$ ), instead, depends only on the rotational kinetic energy of spacecraft [see Eq. (12)]. Both potential functions (11) and (12), being quadratic functions in  $\delta$  and  $\|\boldsymbol{\omega}\|$ , always assume non-negative values and vanish only if  $\delta = 0$  and  $\|\boldsymbol{\omega}\| = 0$ , that is, when the spacecraft angular velocity is zero and the scientific payload axis is aligned with the target direction.

The terms in Eq. (11) inversely proportional to the square of the angular distance between the scientific payload line-of-sight and the undesired space directions, create high potential regions. These latter, when used in conjunction with an appropriate control law, are able to guarantee that the constraints (1) and (2) are met along the whole spacecraft trajectory. In particular, the expressions of  $f_\gamma$  and  $f_i$  for  $\gamma > \hat{\gamma}$  and  $\delta_i < \hat{\delta}_i$  are introduced in Eq. (13) to push the state away from the forbidden region and avoid that a failure in the attitude control system causes the spacecraft to violate the geometric constraints (1)–(2).

Having defined the potential function  $V$ , it is now necessary to evaluate its time derivative. Bearing in mind Eqs. (10)–(12) and recalling Eq. (9), the rate of change of  $V$  is given by:

$$\dot{V} = [\boldsymbol{\omega}]^T \mathbb{E}^T (\nabla V_\delta)^T + \frac{1}{\eta M^{\max}} [\boldsymbol{\omega}]^T \mathbb{I} [\dot{\boldsymbol{\omega}}] \quad (15)$$

where

$$\nabla V_\delta \triangleq \left[ \frac{\partial V_\delta}{\partial q_0}, \frac{\partial V_\delta}{\partial q_1}, \frac{\partial V_\delta}{\partial q_2}, \frac{\partial V_\delta}{\partial q_3} \right]$$

A nonlinear control law can be developed to enforce the condition

$$\dot{V} = -k [\boldsymbol{\omega}]^T [\boldsymbol{\omega}] \quad (16)$$

where  $k > 0$  is a control gain to be chosen such that  $\dot{V}$  is negative semi-definite. Note that  $\dot{V} = 0$  implies that the spacecraft has reached the target condition (that is,  $\delta = 0$  and  $\|\boldsymbol{\omega}\| = 0$ ) or is at a saddle point. Although isolated saddle points may occur, usually these are unstable points<sup>(14)</sup> that cannot trap the system. Therefore, according to the global invariant set theorem<sup>(19)</sup>, the spacecraft trajectory globally asymptotically converges to the desired (target) state.

Extensive simulations have highlighted the presence of saddle points when the number of

geometric constraints is moderate (typically two or three forbidden cones). For topologically complex regions, caused by the intersection of a number of forbidden conical constraints, overlapping potential barriers could be created in regions that are not filled by an actual physical constraint. In general this phenomenon tends to reduce (or even to prevent) the rate of convergence of spacecraft dynamics toward the target direction. However, this is usually a temporary problem because the space position of the forbidden cones varies with time.

Return now to the problem of autonomous reorienting maneuver and consider the control law

$$[\mathbf{M}] = -\eta k M^{\max} [\boldsymbol{\omega}] - \eta M^{\max} \mathbb{E}^T (\nabla V_\delta)^T + \Omega \mathbb{I} [\boldsymbol{\omega}] \quad (17)$$

Recalling Eq. (7), the previous control law is shown to guarantee that  $\dot{V}$  meets Eq. (16) as long as no saturation occurs. In particular, the independent parameters  $\eta$  and  $k$  permit to tune the relative importance of the three terms in Eq. (17). However, when the required control torques are outside the thruster operating range<sup>(14)</sup> (saturation condition), Eq. (17) cannot be used, and is modified as<sup>(14)</sup>

$$M_i = \text{sign}(M_i) M_i^{\max} \quad \text{if} \quad |M_i| > M_i^{\max} \quad \text{with} \quad i = \{x, y, z\} \quad (18)$$

where  $\text{sign}(\cdot)$  is the signum function. Because stability is not guaranteed in the presence of control saturation, extensive simulations are needed to validate the control law in a real mission scenario. In this case a different approach, which involves a backstepping technique, has been recently proposed<sup>(20)</sup> to reduce both the peak control torque and the reorientation time interval.

We are now in a position to better discuss the effect of  $\lambda_1$  and  $\lambda_2$  in Eq. (11). The introduction of  $\lambda_2 > 0$  implies that the potential function cannot take an infinite value and,

at the same time, it is useful to shape the artificial potential slope. This is important because an excessive value of the artificial potential slope would be unmanageable from the control law viewpoint. Indeed, as is shown by Eq. (17), a high value of  $\nabla V_\delta$  implies a control torque that cannot be supplied by the attitude propulsion system, due to the thruster's operational constraints (18). On the other hand, the parameter  $\lambda_1 > 0$  allows one to scale the artificial potential function and to limit its maximum value. In fact, high potential values would cause unwanted overlapping phenomena, especially in the boundary regions around the undesired space orientations. This in turn would create space regions with high potential that would be almost unattainable by the spacecraft.

## Variable Gain Control

The characteristics of the spacecraft response, whose control law is described by Eqs. (17)-(18), are strongly dependent on the choice of the design parameter  $k$ . In particular, assuming that the torque level is within its operational range and substituting Eq. (7) into (17), the spacecraft angular velocity may be expressed as

$$[\dot{\boldsymbol{\omega}}] + k \eta M^{\max} \mathbb{I}^{-1} [\boldsymbol{\omega}] + \eta M^{\max} \mathbb{I}^{-1} \mathbb{E}^T (\nabla V_\delta)^T = 0 \quad (19)$$

Using a sufficiently high value of  $k$ , such that  $k \eta M^{\max} / I^{\min} \gg 1$  and  $k \|\boldsymbol{\omega}\| \gg \|\mathbb{E}^T (\nabla V_\delta)^T\|$  (where  $I^{\min} \triangleq \min \{I_x, I_y, I_z\}$ ), Eq. (19) is approximated by

$$[\dot{\boldsymbol{\omega}}] + k \eta M^{\max} \mathbb{I}^{-1} [\boldsymbol{\omega}] \approx 0 \quad (20)$$

The resulting dynamics is characterized by a fast angular velocity reduction. Indeed, the spacecraft's rotational motion is equivalent to that of a first order system with a small time constant. This behavior is well suited during the pointing terminal phase, when the payload

line-of-sight is nearly aligned with the target direction (more precisely when  $\delta < \delta_{\text{th}}$ , where  $\delta_{\text{th}}$  is a given threshold value of the slew angle), and the rotational velocity modulus is sufficiently small. In fact, in such a situation the angular velocity should be quickly set to zero in order to stop the spacecraft rotational motion at the desired target attitude.

It should be noted that a high value of  $k$  cannot be used when the scientific payload axis is far from the target direction, and the rotational velocity modulus is not sufficiently small, otherwise either a control input saturation occurs or an undesired slowing down of the spacecraft reorientation maneuver takes place. The reason is that when the angular velocity is high, such that the propulsion system torque is saturated, Eqs. (17) and (18) state that  $\mathbf{M}$  is essentially in opposite direction with respect to  $\boldsymbol{\omega}$ . This characteristic tends to slow down the spacecraft rotational motion regardless of the value of  $\delta$  (that is, the angular distance of payload axis from the target direction).

On the other hand, too small a value of  $k$  would cause the violation of the pointing constraints (1)-(2). In fact, because the thruster torques cannot exceed a maximum value, the spacecraft must avoid approaching a pointing constraint with a high angular velocity, otherwise the control system would be unable to arrest the spacecraft before the constraint is violated. To further investigate this point it is useful to estimate the time interval  $T_i$  needed by the control system to set to zero the spacecraft angular velocity about its  $i$ -th principal axes (with  $i = \{x, y, z\}$ ), starting from an initial angular velocity  $\omega_{i_0} \neq 0$ .

The minimum time interval  $T_i$  is obtained when the absolute value of the control torque is at maximum, i.e., when  $|M_i| = M_i^{\text{max}}$ . In that case  $T_i = I_i \omega_{i_0} / M_i^{\text{max}}$ , see Sidi<sup>(21)</sup>. Correspondingly, the absolute value of the generic rotation angle  $\Delta\theta_i$ , which the spacecraft performs before the angular velocity modulus is zeroed, is given by

$$\Delta\theta_i = -\frac{M_i^{\text{max}} T_i^2}{2 I_i} + \omega_{i_0} T_i = \frac{\omega_{i_0}^2 I_i}{2 M_i^{\text{max}}} \leq \frac{\omega_0^2 I^{\text{max}}}{2 M^{\text{min}}} \quad (21)$$

where  $I^{\max} \triangleq \max \{I_x, I_y, I_z\}$ ,  $\omega_0 \triangleq \|\boldsymbol{\omega}(t_0)\|$ , and  $M^{\min} \triangleq \min \{M_x^{\max}, M_y^{\max}, M_z^{\max}\}$ . To avoid that during the slowing down maneuver the scientific payload axis may violate the pointing constraints, it is sufficient to enforce the condition

$$\frac{\omega_0^2 I^{\max}}{2 M^{\min}} \leq \delta^{\min} \triangleq \min \left\{ |\delta_1 - \hat{\delta}_1|, \dots, |\delta_m - \hat{\delta}_m| \right\}_{t=t_0} \quad (22)$$

Dropping the dependence on  $t_0$  (which is a generic time instant) the preceding equation provides an estimate of the maximum acceptable value of the actual spacecraft's angular velocity modulus  $\omega = \|\boldsymbol{\omega}\|$  during the reorientation maneuver, viz.

$$\omega \leq \omega_{\max} \triangleq \sqrt{\frac{2 M^{\min} \delta^{\min}}{I^{\max}}} \quad (23)$$

In other terms, the spacecraft cannot exceed a certain angular velocity (or rotational kinetic energy) given by inequality (23), otherwise the control system is unable to safely arrest its maneuver when a geometric pointing constraint is going to be violated (note, however, that Eq. (23) is a sufficient condition).

The above considerations suggest using a variable control gain  $k$  whose instantaneous value depends both on the actual slew angle  $\delta$  and on the spacecraft angular velocity modulus  $\omega$ . More precisely, the suggested control law is as follows:

$$k = \begin{cases} k_h & \text{if } (\delta < \delta_{\text{th}}) \cup (\omega \geq \sqrt{2 M^{\min} \delta^{\min} / I^{\max}}) \\ k_l & \text{otherwise} \end{cases} \quad (24)$$

where  $k_h \gg k_l$  is a high gain value that guarantees a sharp drop of spacecraft angular velocity near the target direction or a forbidden region. Of course, Eq. (24) makes  $k$  to be time dependent. However, to simplify its practical implementation, the value of  $k$  may be

updated only at constant time intervals of length  $\Delta t$ .

## Numerical Simulations

A large angle reorientation maneuver for a space telescope is now illustrated using the previous methodology. In particular, the geometric-inertial data of the Infrared Space Observatory (ISO) are considered<sup>(16,22)</sup>, whose principal moments of inertia are  $I_x = 6587 \text{ kg m}^2$ ,  $I_y = 7526 \text{ kg m}^2$  and  $I_z = 3813 \text{ kg m}^2$ . The control torques are assumed in the range  $M_x \in [-2.8, 2.8] \text{ N m}$ , whereas  $M_y$  and  $M_z$  are within  $[-3.6, 3.6] \text{ N m}$ . These values are representative of thruster pairs mounted on the telescope periphery and capable of providing a maximum thrust of about 1 N. These values are consistent with those discussed in Ref. [13].

Assume that  $\mathbf{n}_P \equiv \mathbf{k}$  and  $\mathbf{n}_{SA} \equiv \mathbf{i}$ , and consider the pointing constraints due to Sun, Earth, Moon and Jupiter. Recalling Fig. 1 and Eq. (1), the maximum solar array sun angle and the aperture of the forbidden cone are shown in Table 1. The latter also defines the gains of the control law, such as  $k_h$  and  $k_l$ , which have been chosen with a trial and error procedure. A set of simulations are necessary to obtain a satisfactory result, because the control law performances are affected by the value of the selected gains. Note that the angular constraints for the reference spacecraft are compatible with the requirements of a typical infrared telescope<sup>(22)</sup>.

A slewing rest-to-rest ( $\omega_{x_0} \equiv \omega_{y_0} \equiv \omega_{z_0} = 0$ ) maneuver of near 113 deg has been simulated, where the target is particularly difficult to be reached because its position is near the intersection of two forbidden cones (see Fig. 2). At the beginning of the reorientation maneuver, the components in the inertial reference frame  $\mathcal{T}_I$  of the scientific payload axis



parameter	value	units
$k_h$	1000	
$k_l$	1	
$I^{\max}$	7526	kg m <sup>2</sup>
$M^{\max}$	3.6	N m
$M^{\min}$	2.8	N m
$\Delta t$	10	s
$\eta$	1	
$\lambda_1$	1	
$\lambda_2$	0.01	
$\widehat{\gamma}$	30	deg
$\delta_{\text{th}}$	5	deg
$\widehat{\delta}_{\odot}$	27	deg
$\widehat{\delta}_{\oplus}$	65	deg
$\widehat{\delta}_{\zeta}$	24	deg
$\widehat{\delta}_{\gamma_+}$	7	deg

**Table 1: Geometric and control law data.**

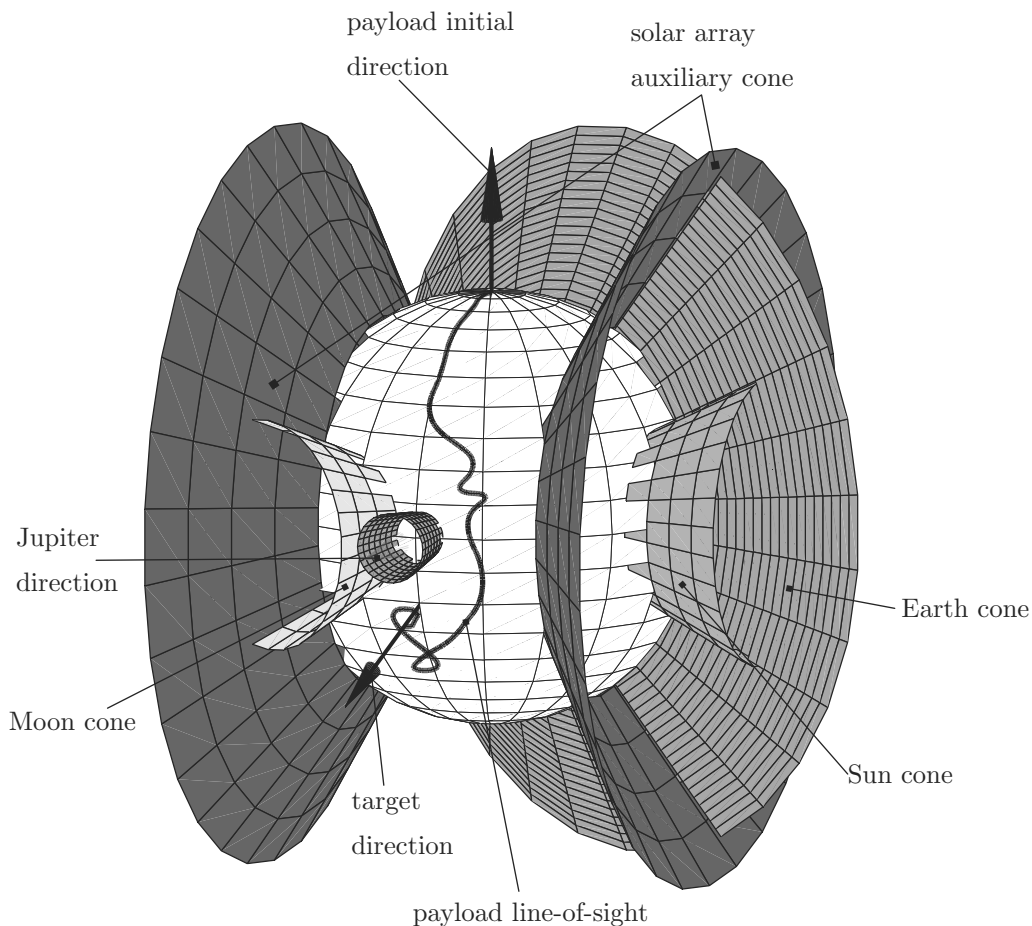
$\mathbf{n}_P$ , the forbidden directions, and the target position  $\mathbf{n}_*$  are

$$[\mathbf{n}_P]_{\mathcal{T}_I} = \begin{bmatrix} 0 \\ 0 \\ 1 \end{bmatrix}, \quad [\mathbf{n}_{\odot}]_{\mathcal{T}_I} = \begin{bmatrix} 1 \\ 0 \\ 0 \end{bmatrix}, \quad [\mathbf{n}_{\zeta}]_{\mathcal{T}_I} = -0.5 \begin{bmatrix} 1 \\ \sqrt{3} \\ 0 \end{bmatrix} \quad (25)$$

$$[\mathbf{n}_{\oplus}]_{\mathcal{T}_I} = 0.5 \begin{bmatrix} 1 \\ \sqrt{3} \\ 0 \end{bmatrix}, \quad [\mathbf{n}_{\gamma_+}]_{\mathcal{T}_I} = \begin{bmatrix} 0 \\ 1 \\ 0 \end{bmatrix}, \quad [\mathbf{n}_*]_{\mathcal{T}_I} = - \begin{bmatrix} 0.0958 \\ 0.8962 \\ 0.433 \end{bmatrix} \quad (26)$$

Since the unit vectors  $\mathbf{n}_P$  and  $\mathbf{n}_{SA}$  are assumed to be orthogonal, the solar array cones drawn in Fig. 2 are the auxiliary cones generated around the Sun-spacecraft direction with semi-aperture angles equal to  $\beta \triangleq (90 \text{ deg} - \widehat{\gamma})$ . These are useful to visualize the exclusion cones for the payload pointing direction associated with the solar array cone within which the

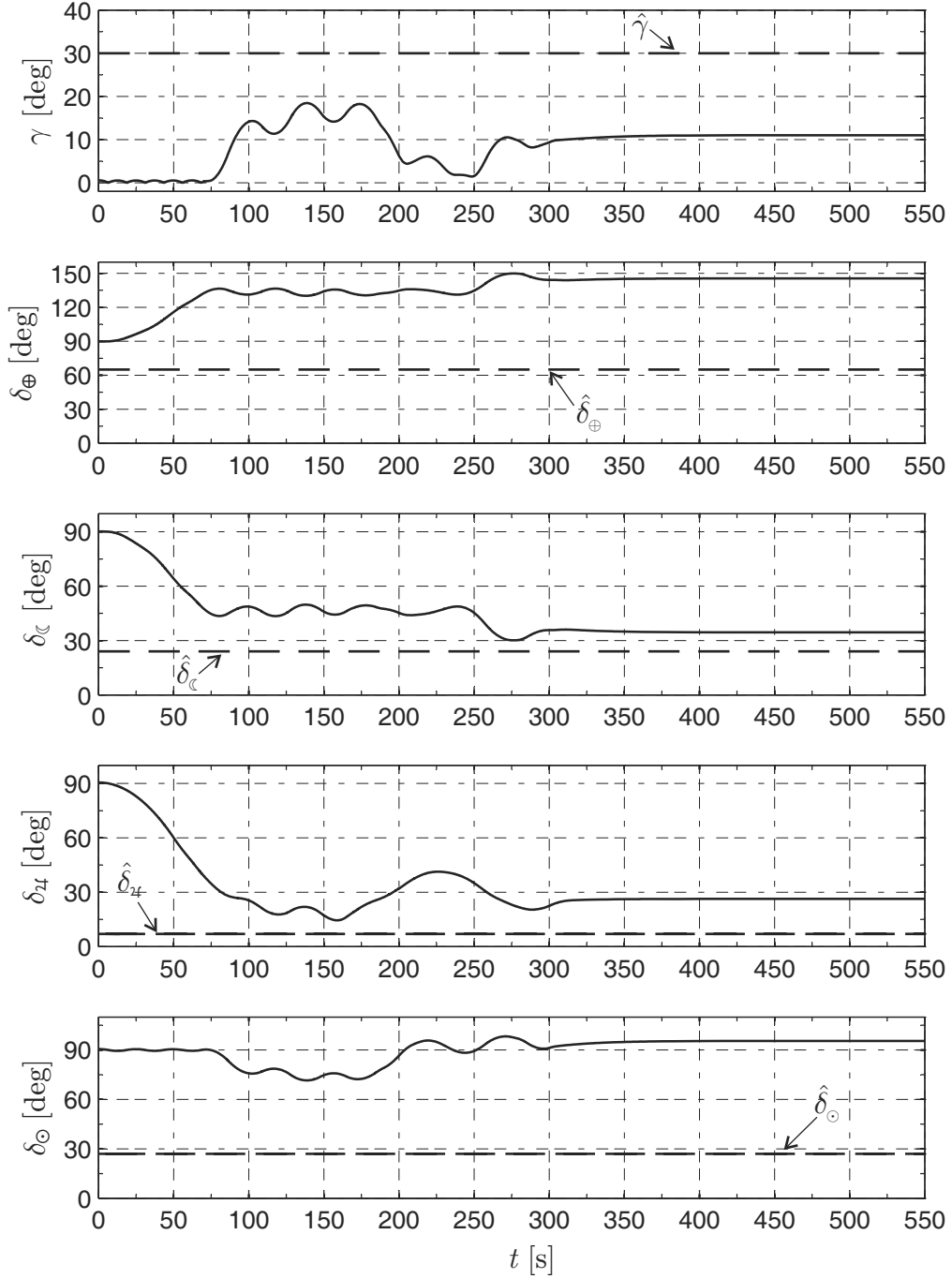
vector  $\mathbf{n}_{SA}$  is constrained to lie. Figure 2 also shows the payload line-of-sight time history. It is clear that all the constraints are met along the spacecraft reorientation trajectory. The effectiveness of the control system is better appreciated with the aid of Fig. 3, where the plots of  $\delta_{\oplus}$ ,  $\delta_{\zeta}$ ,  $\delta_{\eta}$ , and  $\delta_{\odot}$  show that they keep above the specified minimum values.



**Figure 2:** Sketch of the spacecraft reorientation maneuver with the payload initial direction, the target direction and the visible constraints.

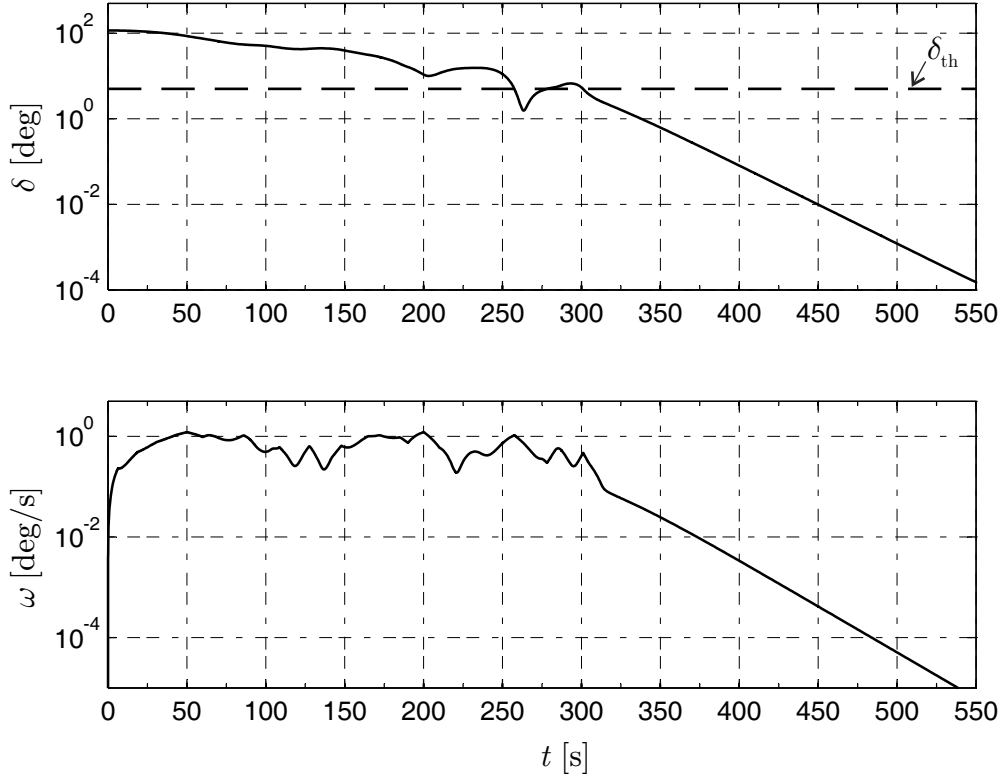
Figure 4 illustrates the slew angle  $\delta$  and the modulus of the spacecraft angular velocity  $\omega$ . It should be noted that, at the end of the maneuver, both constraints are met. In particular the slew angle becomes smaller than  $1 \times 10^{-2}$  deg in about 450 s.

Figure 5 shows the variations of the control gain  $k$  with time as well as the time histories of the components of the control torque  $\mathbf{M}$  in the body reference frame  $\mathcal{T}_B$ . In particular,



**Figure 3:** Time variation of angles  $\gamma$ ,  $\delta_{\oplus}$ ,  $\delta_{\zeta}$ ,  $\delta_{\eta}$ , and  $\delta_{\odot}$  during the slew maneuver.

the grey zones in the time history of  $k$  have been added to highlight the time intervals within which  $\omega > \omega_{\max}$ , see Eq. (23). During these time intervals  $k$  is at maximum (recall Eq. (24)), the command torque is saturated and the spacecraft tends to decelerate the rotational motion



**Figure 4:** Semi-logarithmic plots of slew angle and spacecraft angular velocity as a function of time.

see Fig. 4.

Note the final increase of  $k$  that occurs when the slew angle achieves the threshold value  $\delta_{\text{th}}$ , see Fig. 4. In this situation the spacecraft quickly sets to zero its angular velocity following a first-order dynamics, in accordance with Eq. (20). Also note that a saturation exists in all of the control torque components.

## Conclusions

A new methodology has been developed to handle large angle slew maneuvers with pointing constraints. The problem of attitude control has been formulated and solved through artificial potential functions, thus considerably simplifying the spacecraft reorientation maneuvers with autonomous re-targeting capabilities. Unlike the usual approaches available in the literature, a time variant control gain is chosen to reduce the duration of the reorienta-

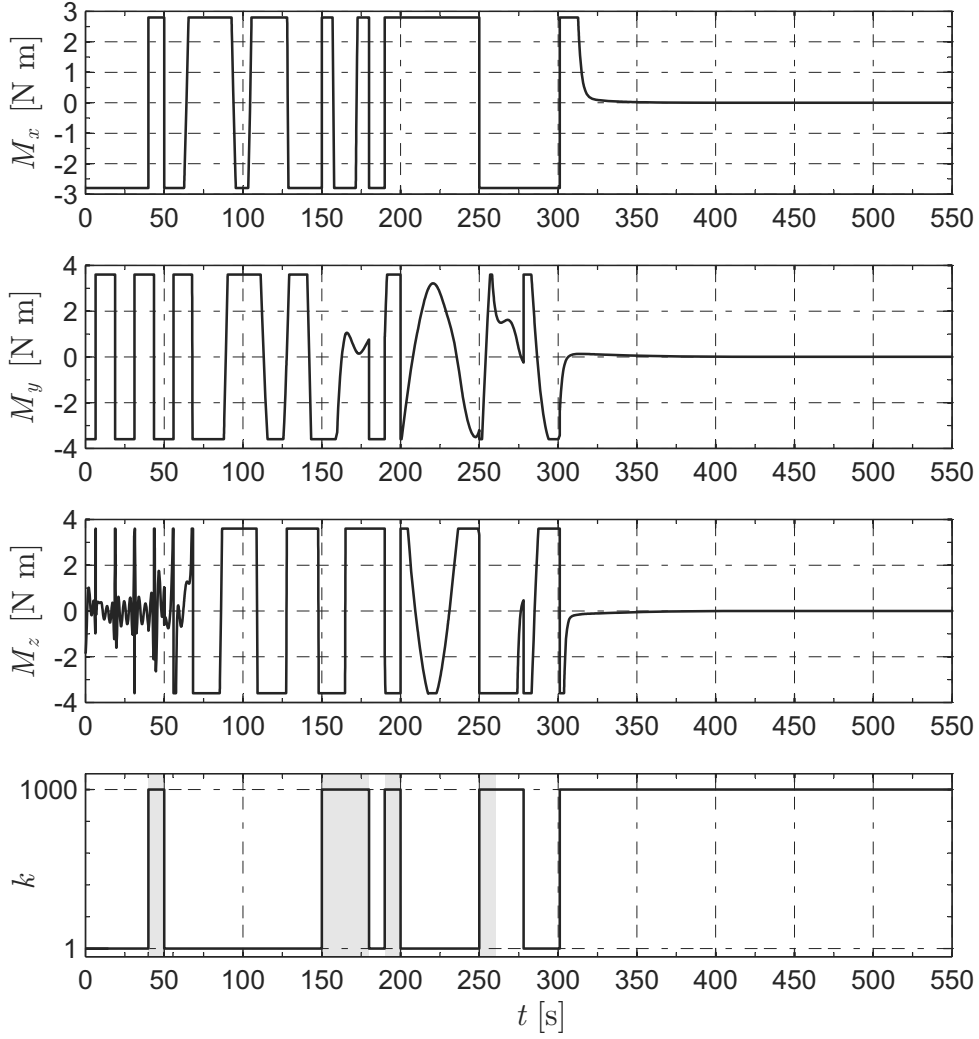


**Figure 5:** Time histories of control torques  $M_x$ ,  $M_y$  and  $M_z$ , and the control gain  $k$ .

tion maneuver. The rationale is that high values of the control gain correspond to a slow spacecraft movement, whereas small values of  $k$  give rise to rapid reorientation maneuvers. The control gain value depends both on the system kinetic energy and on the distance of the spacecraft from the target direction. As a result, close connections between the control law and fundamental physical quantities are established. More important, the spacecraft is able to reach points in the potential field arbitrarily close to a constraint and to maneuver with autonomous capability of guidance and control. Accordingly, autonomous avoidance of undesired space orientations is obtained and constraints due to the solar array pointing

requirements are met.

## References

1. Kumar, R. R., “Artificial Neural Networks in Space Station Optimal Attitude Control,” *World Space Congress*, Washington DC, 27 August - 4 September 1992, Paper IAF-92-0038.
2. Frakes, J. P., Henretty, D. A., Flatley, T. W., Markley, L. F., San, J. K., and Lightsey, E. G., “SAMPEX Science Pointing with Velocity Avoidance,” *AAS/AIAA Spaceflight Mechanics Meeting*, Colorado Springs, CO (USA), February 24–26 1992, Paper AAS 92-182.
3. Singh, G., Macala, G., Wong, E. C., and Rasmussen, R. D., “A Constraint Monitor Algorithm for the Cassini Spacecraft,” *AIAA Guidance, Navigation, and Control Conference*, New Orleans, LA, August 1997, Paper AIAA 97-3526.
4. Sørensen, A. M., “ISO Attitude Maneuver Strategies,” *Advances in the Astronautical Sciences*, Vol. 84, 1993, pp. 975–987.
5. Wie, B. and Barba, P. M., “Quaternion Feedback for Spacecraft Large Angle Maneuvers,” *Journal of Guidance, Control, and Dynamics*, Vol. 8, No. 3, May-June 1985, pp. 360–365. doi: 10.2514/3.19988.
6. Bilimoria, K. D. and Wie, B., “Time-Optimal Three-Axis Reorientation of a Rigid Spacecraft,” *Journal of Guidance, Control, and Dynamics*, Vol. 16, No. 3, May-June 1993, pp. 446–452. doi: 10.2514/3.21030.
7. Shen, H. and Tsiotras, P., “Time-Optimal Control of Axisymmetric Rigid Spacecraft Using Two Controls,” *Journal of Guidance, Control, and Dynamics*, Vol. 22, No. 5, September-October 1999, pp. 682–694. doi: 10.2514/2.4436.
8. Liu, S. W. and Singh, T., “Fuel/Time Optimal Control of Spacecraft Maneuvers,” *Journal of Guidance, Control, and Dynamics*, Vol. 20, No. 2, March-April 1997, pp. 394–397. doi: 10.2514/2.4053.

9. Bryson, A. E. and Ho, Y. C., *Applied Optimal Control*, chap. 2, Hemisphere Publishing Corporation, New York, NY, 1975, pp. 117–125, ISBN: 0-891-16228-3.
10. Melton, R. G., “Hybrid Methods for Determining Time-Optimal, Constrained Spacecraft Reorientation Maneuvers,” *IAA Conference on Dynamics and Control of Space Systems*, Porto, Portugal, March 2012, Paper IAA-AAS-DyCoSS1-07-08.
11. Melton, R. G., “Numerical Analysis of Constrained, Time-Optimal Satellite Reorientation,” *Mathematical Problems in Engineering*, Vol. 2012, 2012, pp. 1–19, Article ID 769376. doi: 10.1155/2012/769376.
12. McInnes, C. R., “Potential Function Methods for Autonomous Spacecraft Guidance and Control,” *AAS/AIAA Astrodynamics Specialist Conference*, Halifax, Nova Scotia, Canada, August 1995, Paper AAS 95-447.
13. McInnes, C. R., “Large Angle Slew Manoeuvres with Autonomous Sun Vector Avoidance,” *Journal of Guidance, Control and Dynamics*, Vol. 17, No. 4, July-August 1994, pp. 875–877. doi: 10.2514/3.21283.
14. Radice, G. and McInnes, C. R., “Constrained On-Board Attitude Control Using Gas Jet Thrusters,” *The Aeronautical Journal*, Vol. 103, No. 1030, December 1999, pp. 549–556.
15. Casasco, M. and Radice, G., “Autonomous Slew Manoeuvring and Attitude Control Using the Potential Function Method,” *Advances in the Astronautical Sciences*, Vol. 116, 2003, pp. 1745–1765.
16. Mengali, G. and Quarta, A. A., “Spacecraft control with constrained fast reorientation and accurate pointing,” *The Aeronautical Journal*, Vol. 108, No. 1080, February 2004, pp. 85–91.
17. Hablani, H. B., “Attitude Commands Avoiding Bright Objects and Maintaining Communication with Ground Station,” *Journal of Guidance, Control, and Dynamics*, Vol. 22, No. 6, November-December 1999, pp. 759–767. doi: 10.2514/2.4469.

18. Meyer, G., “Design and Global Analysis of Spacecraft Attitude Control Systems,” Tech. rep., NASA, March, 1 1971, NASA TR-R-361.
19. Slotine, J.-J. E. and Li, W., *Applied Nonlinear Control*, Prentice Hall, Englewood Cliffs, NJ, 1991, pp. 73–74, ISBN: 0-130-40890-5.
20. Ali, I., Radice, G., and Kim, J., “Backstepping Control Design with Actuator Torque Bound for Spacecraft Attitude Maneuver,” *Journal of Guidance, Control and Dynamics*, Vol. 33, No. 1, January-February 2010, pp. 254–259. doi: 10.2514/1.45541.
21. Sidi, M. J., *Spacecraft Dynamics and Control: A Practical Engineering Approach*, Cambridge University Press, New York, NY, 1997, pp. 140–141, ISBN: 0-521-78780-7.
22. Leech, K. and Pollock, A. M. T., “ISO - The Satellite and its Data,” Volume II SAI/99-082/Dc, Space Science Department of ESA, Villafranca, P.O. Box 50727, E-28080 Madrid, Spain, July 2000, Version 1.0.